Hooman & Gurgenci ASME-J. Heat Transfer 130 (1) 012501 (2008) (*6 pages*)

Heatline visualization of natural convection in a porous cavity occupied by a fluid with temperature dependent viscosity

K. Hooman, H. Gurgenci

School of Engineering, The University of Queensland, Brisbane, QLD 4072, Australia

Tel: +61 7 33653668 Fax: +61 7 33654799 E-mail: K.hooman@uq.edu.au

Abstract

Temperature dependent viscosity effect in buoyancy driven flow, of a gas or a liquid, in an enclosure filled with a porous medium is studied numerically, based on the general model of momentum transfer in a porous medium. The Arrhenius model, which proposes an exponential form of viscosity-temperature relation, is applied to examine three cases of viscosity-temperature relation: constant, decreasing and increasing. Application of arithmetic and harmonic mean values of the viscosity is also investigated for their ability to represent the Nusselt number versus the effective Rayleigh number. Heatlines are illustrated for a more comprehensive investigation of the problem.

Keywords: Natural convection, Heatline visualization, Porous media, Variable property, Numerical, Non-Darcy

Nomenclature

b	viscosity variation number
C_F	inertia coefficient
Da	the Darcy number, $Da=K/L^2$
g	gravitational acceleration
H*	heatfunction
H	dimensionless heatfunction
k	porous medium thermal conductivity
K	permeability
L	cavity height
Nu	the Nusselt number
P*	pressure

Pr_c modified Prandtl number, $\mathrm{Pr}_c = \phi\nu_c / \alpha$

q'' heat flux

R maximum streamfunction ratio, $R=\psi_{max}/\psi_{max,cp}$

Ra_f the Rayleigh number, $Ra_f=g\beta L^4 q''/(\nu_c \alpha k)$

Ra Rayleigh-Darcy number, $\mathrm{Ra}=\mathrm{Ra}_f/s^2$.

$Ra_{\Delta T}$ the Rayleigh number based on ΔT, $Ra_{\Delta T}=g\beta\Delta T\, L^3/(\nu_c \alpha)$

s porous media shape parameter, $s=Da^{-1/2}$

S_φ source term for φ equation

S_ω source term for vorticity transport equation

T^* temperature

T_c cold wall temperature

u^* x*-velocity

(u, v) (u*,v*)L/α

$|U^*|$ mean velocity $(u^{*2}+v^{*2})^{1/2}$

$|U|$ dimensionless mean velocity $(u^2+v^2)^{1/2}$

v^* y*-velocity

x^*,y^* horizontal and vertical coordinate

(x,y) $(x^*,y^*)/L$

Greek symbols

α thermal diffiusivity of the porous medium

β thermal expansion coefficient

Γ_φ diffusion parameter

Λ inertial parameter $\Lambda = C_F L\phi^2 /(\mathrm{Pr}_c \sqrt{K})$

θ dimensionless temperature

η kinematic viscosity ratio

μ fluid viscosity

ν	kinematic viscosity
ρ	fluid density
Ψ	stream function
φ	generic variable
ϕ	porosity
ω	vorticity

subscript

am	arithmetic mean
ave	average
C	of cold wall
cp	constant property
eff	effective
H	of hot wall

1. INTRODUCTION

Most previous studies on free convection in porous media assumed the viscosity of the fluid to be constant. However, there are special cases where the viscosity changes with temperature while other fluid properties remain relatively constant, see for example [1]. On the other hand, variable-property free convection in a porous cavity has been analyzed by some authors as surveyed by Nield and Bejan [2].

Nield [3, 4] argued that property variation should not affect convection if one uses an effective Rayleigh number based on mean values. Chu and Hickox [5] reported that even extreme viscosity variations did not have a significant effect on the overall free convection heat transfer coefficient provided the properties were evaluated at the arithmetic mean temperature and a correction factor was used. Siebers et al. [6] have come up with similar conclusion for free convection of air along a vertical plate.

On the other hand, applying the general model of Vafai and Tien [7] and Hsu and Cheng [8], Guo and Zhao [9] numerically studied natural convection of PAO, a poly-alpha-olefin with a temperature-dependent viscosity, and predicted a higher Nusselt number when the viscosity decreased with the temperature. With properties evaluated at the arithmetic mean temperature (of hot and cold walls), their results still showed significant differences between constant- and variable-property flows. For example, for $Da=10^{-4}$ and $Ra=10$, their Nu was about 75% higher than Nu_{cp}.

Apparently, more investigation is needed to study the effect of temperature-dependent viscosity on natural convection. This work addresses the issue by considering a square porous cavity, depicted in Fig. 1, similar to that of [10-12]. Following recommendations by [13], the Arrhenius model for viscosity-temperature relation is applied here for flow of an incompressible fluid. The viscosity of a gas usually increases with temperature and the viscosity of a liquid does the reverse. We consider both cases.

Previous work on the effects of property variation on convection heat transfer, in fluids clear of solid material, has been surveyed by Kakaç [14]. Recently, Narasimhan and Lage [1] have reviewed the issue for forced convection in a porous duct.

2. MODEL EQUATIONS

Incompressible natural convection of a fluid with temperature-dependent viscosity in a square enclosure filled with homogeneous, saturated, isotropic porous medium with the Oberbeck–Boussinesq approximation for the density variation in the buoyancy term is considered, as shown in Fig. 1-a. Solid matrix and the fluid are in local thermal equilibrium. The governing equations can be written as

$$\frac{\partial(u^*\varphi)}{\partial x^*}+\frac{\partial(\mathrm{v}^*\varphi)}{\partial y^*}=\frac{\partial}{\partial x^*}(\Gamma_\varphi\frac{\partial\varphi}{\partial x^*})+\frac{\partial}{\partial y^*}(\Gamma_\varphi\frac{\partial\varphi}{\partial y^*})+S_\varphi \qquad (1)$$

where φ stands for the dependent variables u^*, v^*, T^*; and Γ_φ, S_φ are the corresponding diffusion and source terms, respectively, for the general variable φ, as summarized in table 1.

The Arrhenius model assumes

$$\eta=\nu/\nu_c=\exp(b\theta), \qquad (2)$$

where b is positive/negative in case of a gas/liquid whose viscosity increases/decreases with an increase in temperature. Our dimensionless temperature is $\theta=k(T^*-T_c)/(q''L)$ following Bejan [15]'s recommendation to select the lowest temperature as the reference temperature for heatline visualization purposes. One also notes that the Taylor series expansion for very small values of b leads to linear or inverse linear ν-θ relation as

$$\begin{aligned}\nu&=\nu_c(1+b\theta),\\ \nu^{-1}&=\nu_c^{-1}(1-b\theta),\end{aligned} \qquad (3\text{-a,b})$$

similar to [16-19].

The dimensionless stream-function is defined as

$$\begin{aligned}u&=\partial\psi/\partial y,\\ \mathrm{v}&=-\partial\psi/\partial x.\end{aligned} \qquad (4\text{-a,b})$$

Taking the curl of *x**- and *y**-momentum equations and eliminating the pressure terms, one has

$$u.\nabla\omega = \mathrm{Pr}_c((\nabla^2\omega - s^2\omega)e^{b\theta} - \Lambda|U|\omega + S_w) \tag{5}$$

where

$$S_w = s^2(\frac{\partial\eta}{\partial x}\frac{\partial\psi}{\partial x} + \frac{\partial\eta}{\partial y}\frac{\partial\psi}{\partial y}) + \Lambda(\frac{\partial|U|}{\partial x}\frac{\partial\psi}{\partial x} + \frac{\partial|U|}{\partial y}\frac{\partial\psi}{\partial y}) + Ra_f\frac{\partial\theta}{\partial x}$$
$$-(\frac{\partial}{\partial y}(\frac{\partial\eta}{\partial x}\frac{\partial^2\psi}{\partial x\partial y} + \frac{\partial\eta}{\partial y}\frac{\partial^2\psi}{\partial y^2}) + \frac{\partial}{\partial x}(\frac{\partial\eta}{\partial x}\frac{\partial^2\psi}{\partial x^2} + \frac{\partial\eta}{\partial y}\frac{\partial^2\psi}{\partial x\partial y})). \tag{6}$$

The vorticity directed in *z* direction is defined as

$$\omega = -\nabla^2\psi\,. \tag{7}$$

The thermal energy equation now takes the following form

$$u.\nabla\theta = \nabla^2\theta\,. \tag{8}$$

The Nusselt number, following Merrikh and Mohamad [11], is defined as actual heat transfer divided by pure conduction as

$$Nu = 1/\theta_{wall,ave},$$
$$\theta_{wall,ave} = \int_0^1\theta(0,y)dy. \tag{9-a,b}$$

where $\theta_{wall,ave}$ is the average dimensionless temperature measured over the left (heated) wall. Following Bejan [15], the *heatfunction* concept is applied, which is an invention similar to streamfunction but more suitable to visualise heat transfer. The heatfunction, *H*(x*,y*)*, intrinsically satisfies the thermal energy equation while the streamfunction does the same for the mass continuity equation. Patterns of *H**=constant *heatlines* are lines across which the net flow of energy is zero. Non-dimensional heatfunction is defined as

$$\frac{\partial H}{\partial y} = u\theta - \frac{\partial\theta}{\partial x},$$
$$-\frac{\partial H}{\partial x} = \mathrm{v}\theta - \frac{\partial\theta}{\partial y}. \tag{10-a,b}$$

The problem is now to solve Eqns. (5-10) subject to the boundary conditions shown in Fig. 1-b.

3. NUMERICAL DETAILS

All runs were performed on a 90x90 grid. Our Rayleigh-Darcy number, or simply *Ra* hereafter, is limited to 10^3 while our *Da* ranges from 10^{-6} to 1; and the modified Prandtl number and the inertia parameter are both fixed at unity, similar to [11]. Grid independence was verified by running different combinations of *s*, Ra_f, and *b* on 90x90 and 120x120 grids to observe less than 1% difference between results obtained on different grids. The convergence criterion (maximum relative error in the values of the dependent variables between two successive iterations) was set at 10^{-5}.

According to table 2, our results are close to those of [10, 11, 20] for $Da=10^{-6}$ while table 3 checks our *Nu* at higher *Da* (*Da*=0.01 or *s*=10) against [20]. Their results were for an isothermally heated cavity but, following Bejan [15], one can modify their *Nu-Ra* correlation to compare against a problem with isoflux heating. The Rayleigh number based on temperature difference in an isothermally heated cavity can be related to a heat flux based *Ra*, here Ra_f, as

$$Ra_{\Delta T} = Ra_f / Nu \,. \tag{11}$$

In this way $Nu = CRa_{\Delta T}^m$ reads $Nu = (CRa_f^m)^{\frac{1}{1+m}}$, as noted by Bejan [15] for free convection in a cavity without a porous medium.

4. RESULTS AND DISCUSSION

Fig. 2 shows line diagrams of v(*x*,0.5) and θ(*x*,0.5) for *Ra*=50 with various *b* values. For a constant-property fluid (*b=0*), the velocity peaks near the opposing walls more or less mirror each other. If the viscosity has a decreasing relation with temperature (*b<0*), the absolute value of the peak vertical velocity near the heated wall is higher than its counterpart near the opposing wall (cold wall). With *b>0*, the situation is reversed and the vertical velocity is higher nearer the cold wall. Lower levels of θ are predicted with a decrease in *b*, which may be a manifestation of increased convection equalizing the temperatures as *b* is reduced. Moreover, with *b*=1.5 and *Ra*=50, the dimensionless mid-plane temperature varies almost linearly with *x* that implies a conduction-dominated heat transfer.

Fig. 3 shows the dependence of the Nu/Nu_{cp} and *R* on *b*. The dependence is higher at smaller *Ra*. For the range of variables considered, *Nu* and the stream function vary from their constant-property values by up to 20% and 25%, respectively.

According to Fig. 4, the net energy path consists of two vertical boundary layers connected through an energy tube located along the upper wall. The two walls maintain different boundary conditions and their boundary layers are therefore different. At the isothermal wall, the heatlines are normal to wall. At the isoflux wall, the heatline slope shows the amount of energy transferred from the wall and vertical increments in heatfunctions are constant. As seen, horizontal heatlines imply conduction-dominated heat transfer and this dominance becomes clearer with *b>0*. For example, almost perfectly horizontal heatlines at *b*=1.5 indicates the heat transfer occurring almost entirely by conduction, a situation already observed at this value of *b* by the linear temperature distribution in Fig. 2. The degree of upward deflection of the heatlines represents the strength of convective heat flow, interpreted as 'heat rises' by Bejan [15]. It seems that heatlines can be used to show the onset of convection instead of isotherms. However, investigation of this possibility is left for a future report. As *b* decreases or *s* increases at a fixed value of *Ra*, the heatlines become denser near the top wall that implies higher heat transfer rate.

Nevertheless, this is probably more due to the fact that Ra_f had to be increased to maintain a constant Ra with an increase in s.

The above results demonstrate the apparently destabilizing effect of viscosity decreasing with increased temperature when Ra is calculated at T_c. Let us now see what happens when using average Rayleigh numbers.

Nield [3] recommends using harmonic average for the fluid viscosity in effective Rayleigh number, i.e.

$$Ra_{eff} = (Ra_C + Ra_H)/2 . \tag{12}$$

Applying the average wall temperature for the hot wall, one has

$$Ra_H = Ra \exp(-b/Nu), \tag{13}$$

with $Ra_C=Ra$ it leads to

$$Ra_{eff} = Ra(1+\exp(-b/Nu))/2 . \tag{14}$$

Eq. 14 can be used to find Ra_{eff} only when one knows Nu. This makes its application somehow difficult. However, as a first approximation, one can apply the Nu_{cp} value instead of Nu. It will be shown, by tables 4-5, that this approximation will lead to a maximum error of 6% in Nu.

Table 4 shows a sample of Ra_{eff} for limiting values of b, s, and Ra considered in this study. Also available in this table is Nu/Nu_{cp} calculated in two ways. The first method is application of Ra_{eff} as recommended by Nield [3] with b=0. The Nusselt number then is divided by Nu_{cp} evaluated at $Ra=Ra_C$). This column is labeled as "Estimated" in tables 4-5. The second approach (which was taken so far) is calculating Nu numerically (for a case with non-zero value of b) and then dividing it by its value also numerically calculated at constant property –both calculations done at the same Ra. This column is labeled as "Numerical" in tables 4-5.

As another check on Nield's theory, and based on Eq. (11), we recover the correlations reported by Lauriat and Prasad [20] as

$$\frac{Nu}{Nu_{cp}} = \left(\frac{Ra_{eff}}{Ra}\right)^{\frac{m}{1+m}} . \tag{15}$$

Making use of Eq. (14), Eq. (15) reads

$$\frac{Nu}{Nu_{cp}} = \left(\frac{1+\exp(-b/Nu)}{2}\right)^{\frac{m}{1+m}}, \tag{16}$$

where to the first approximation

$$\frac{Nu}{Nu_{cp}} = \left(\frac{1+\exp(-b/Nu_{cp})}{2}\right)^{\frac{m}{1+m}} . \tag{17}$$

Results of Eq. (17), are shown in table 5 with a procedure similar to that described above concerning the data in table 4. Seemingly, the Ra_{eff} approach works well even when the viscosity ratio can reach as high/low values as 4.5/0.22 while the arithmetic mean value for the viscosity may not be a proper option. For example, applying Eq. (2), Ra_{eff}/Ra_{am} reads

$$\frac{Ra_{eff}}{Ra_{am}} = \left(\frac{1+\exp(-b/Nu)}{2\exp(-b/(2Nu))}\right), \tag{18}$$

where Ra_{am} is the Rayleigh number with the viscosity being evaluated at the arithmetic mean temperature. As $b \to 0$, the Ra ratio tends to 1. However, increasing b, the ratio differs substantially from unity. For example, with s=10 and Ra=100, Nu_{cp}=1.48, based on table 3. With b=3, the Rayleigh ratio becomes 1.56 which leads to a 12 % change in the associate Nu when the correlation by [20] is applied.

5. CONCLUSION

Temperature-dependent viscosity effect on free convection in a porous cavity is studied numerically, based on the general model of momentum transfer in a porous medium. It is found that the effective Rayleigh number works well within the range of the parameters considered here. Applying Ra_{eff}, one can still use the constant property results and this, in turn, will reduce the computational time and expense required for solving a variable-viscosity problem. Moreover, it was observed that application of heatlines gives us a higher resolution as they show lines along which energy is transferred. Dissimilar heatline patterns were observed for different vertical wall boundary conditions. An important parameter is the degree of upward deflection in heatlines as it indicates the heat transfer enhancement. It was also shown that for variable-property free convection in a porous cavity the *Nu-Ra* correlation for isothermal walls can still be modified for isoflux cases. In this way, one can use Nu_{cp} in our Eq (14) instead of Nu (which is unknown and hence can hamper further progress) within a reasonable range of error.

Acknowledgments

The first author, the scholarship holder, acknowledges the support provided by The University of Queensland in terms of UQILAS, Endeavor IPRS, and School Scholarship.

References

[1] Narasimhan, A., Lage, J.L. (2005), "Variable viscosity forced convection in porous medium channels," In *Handbook of Porous Meida*. Ed. Vafai, K., Taylor and Francis, New York, pp. 195-233.

[2] Nield, D.A., Bejan, A., "Convection in porous media," Springer-Verlag, New York 2006.

[3] Nield, D.A. (1994), "Estimation of an Effective Rayleigh Number for Convection in a Vertically Inhomogeneous Porous-Medium or Clear Fluid," *International Journal of Heat and Fluid Flow* **15**: 337-340.

[4] Nield, D.A. (1996), "The effect of temperature-dependent viscosity on the onset of convection in a saturated porous medium," *Journal of Heat Transfer-Transactions of the ASME* **118**: 803-805.

[5] Chu, T.Y., Hickox, C.E. (1990), "Thermal-Convection with Large Viscosity Variation in an Enclosure with Localized Heating," *Journal of Heat Transfer-Transactions of the ASME* **112**: 388-395.

[6] Siebers, D.L., Moffatt, R.F., Schwind, R.G. (1985), "Experimental, Variable Properties Natural-Convection from a Large, Vertical, Flat Surface," *Journal of Heat Transfer-Transactions of the ASME* **107**: 124-132.

[7] Vafai, K., Tien, C.L. (1981), "Boundary and Inertia Effects on Flow and Heat-Transfer in Porous-Media," *International Journal of Heat and Mass Transfer* **24**: 195-203.

[8] Hsu, C.T., Cheng, P. (1990), "Thermal Dispersion in a Porous-Medium," *International Journal of Heat and Mass Transfer* **33**: 1587-1597.

[9] Guo, Z.L., Zhao, T.S. (2005), "Lattice Boltzmann simulation of natural convection with temperature-dependent viscosity in a porous cavity," *Prog. Comput. Fluid Dyn.* **5**: 110-117.

[10] Prasad, V., Kulacki, F.A. (1984), "Natural-Convection in a Rectangular Porous Cavity with Constant Heat-Flux on One Vertical Wall," *Journal of Heat Transfer-Transactions of the ASME* **106**: 152-157.

[11] Merrikh, A.A., Mohamad, A.A. (2002), "Non-Darcy effects in buoyancy driven flows in an enclosure filled with vertically layered porous media," *International Journal of Heat and Mass Transfer* **45**: 4305-4313.

[12] Antohe, B.V., Lage, J.L. (1997), "The Prandtl number effect on the optimum heating frequency of an enclosure filled with fluid or with a saturated porous medium," *International Journal of Heat and Mass Transfer* **40**: 1313-1323.

[13] Harms, T.M., Jog, M.A., Manglik, R.M. (1998), "Effects of temperature-dependent viscosity variations and boundary conditions on fully developed laminar forced convection in a semicircular duct," *Journal of Heat Transfer-Transactions of the ASME* **120**: 600-605.

[14] Kakaç, S. (1987), "The Effect of Temperature-Dependent Fluid Properties on Convective Heat Transfer," In *Handbook of Single-Phase Convective Heat Transfer*. Eds. Kakaç, S., Shah, R.K., Aung, W., Wiley, New York.

[15] Bejan, A.: Convection heat transfer Wiley, Hoboken, N.J. 2004.

[16] Nield, D.A., Porneala, D.C., Lage, J.L. (1999), "A theoretical study, with experimental verification, of the temperature-dependent viscosity effect on the forced convection through a porous medium channel," *Journal of Heat Transfer-Transactions of the ASME* **121**: 500-503.

[17] Nield, D.A., Kuznetsov, A.V. (2003), "Effects of temperature-dependent viscosity in forced convection in a porous medium: Layered-medium analysis,"J. *Porous Media* **6**: 213-222.

[18] Hooman, K. (2006),"Entropy-energy analysis of forced convection in a porous-saturated circular tube considering temperature-dependent viscosity effects," *International Journal of Exergy* **3**: 436–451.

[19] Hooman, K., Gurgenci, H. (2007), "Effects of temperature-dependent viscosity variation on entropy generation, heat, and fluid flow through a porous-saturated duct of rectangular cross-section," *Applied Mathematics and Mechanics (English edition)* **28**: 69 -78.

[20] Lauriat, G., Prasad, V. (1987), "Natural-Convection in a Vertical Porous Cavity - a Numerical Study for Brinkman-Extended Darcy Formulation," *Journal of Heat Transfer-Transactions of the ASME* **109**: 688-696.

Table list

Table 1. Summary of the solved governing equations

Table 2 Present Nu versus those in the literature for s=1000 ($Da=10^{-6}$).

Table 3 Present Nu versus those of [20]for s=10 and $C_F=0$.

Table 4 Calculation of Ra_{eff} and Nu.

Table 5 Calculation of Ra_{eff} and Nu for s=10.

Figure Captions

Fig. 1-a Definition Sketch.

Fig. 1-b Dimensionless boundary conditions

Fig 2 Horizontal mid-plane velocity (top) and temperature (bottom) for different values of b with Ra=50 and s=1000

Fig 3 The variation of Nu/Nu_{cp} (top) and R (bottom) versus b with some values of Ra (s=100).

Fig 4 Heatlines for various b values with Ra=50 and A)s=1, B)s=100, and C) s=1000

Table 1. Summary of the solved governing equations

Equations	φ	Γ_φ	S_φ
Continuity	1	0	0
x*-momentum	u^*/ϕ	ν	$\frac{-1}{\rho}\frac{\partial p^*}{\partial x^*}-\frac{\nu u^*}{K}-\frac{C_F \phi u^* \lvert U^* \rvert}{K^{1/2}}$
y*-momentum	v^*/ϕ	ν	$g\beta(T^*-T_c)-\frac{1}{\rho}\frac{\partial p^*}{\partial y^*}-\frac{\nu v^*}{K}$ $-\frac{C_F \phi v^* \lvert U^* \rvert}{K^{1/2}}$
Energy	T*	α	0

Table 2 Present *Nu* versus those in the literature for s=1000 ($Da=10^{-6}$).

Ra	Present	Ref. [10]	Ref. [11]	Ref. [20]
50	1.57	1.57	-	-
100	2.09	2.09	2.11	1.93
200	2.75	2.78	2.78	2.71
500	3.98	4.06	4.05	3.91
10^3	5.29	5.41	5.35	5.07

Table 3 Present *Nu* versus those of [20]for s=10 and C_F=0.

Ra	Present Nu	Ref. [20]
100	1.48	1.48
200	1.84	1.84
500	2.41	2.42
1000	2.93	2.92

Table 4 Calculation of Ra_{eff} and Nu.

s	b	Ra	Ra_{eff}	Nu/Nu_{cp}	
				Estimated	Numerical
10	-1.5	50	86.02	1.149	1.145
	1.5	50	34.08	0.934	0.91
10^3	-1.5	50	72.25	1.164	1.168
	1.5	50	37.08	0.883	0.833
10	-1.5	10^3	1312.7	1.067	1.07
	1.5	10^3	797.33	0.927	0.923
10^3	-1.5	10^3	1153.05	1.061	1.064
	1.5	10^3	876.35	0.947	0.932

Table 5 calculation of Ra_{eff} and Nu for s=10.

Ra	b	Ra_{eff}	Nu/Nucp	
			Estimated	Numerical
100	-1.5	187.76	1.178	1.152
	1.5	68.15	0.905	0.887
200	-1.5	325.97	1.135	1.113
	1.5	144.25	0.919	0.894
500	-1.5	714.65	1.097	1.08
	1.5	384.51	0.934	0.904
10^3	-1.5	1335.73	1.078	1.076
	1.5	799.14	0.943	0.932

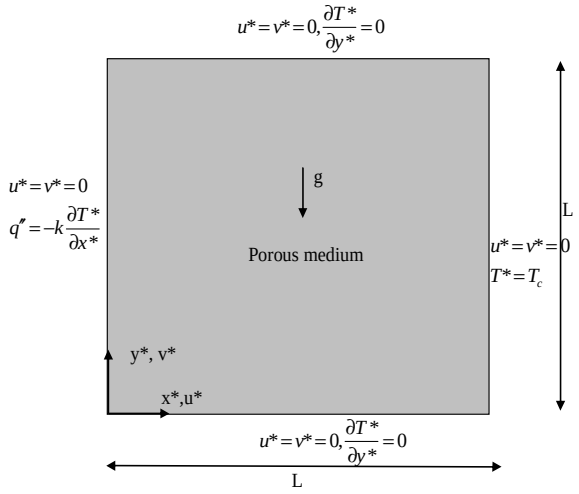

Fig. 1-a Definition Sketch.

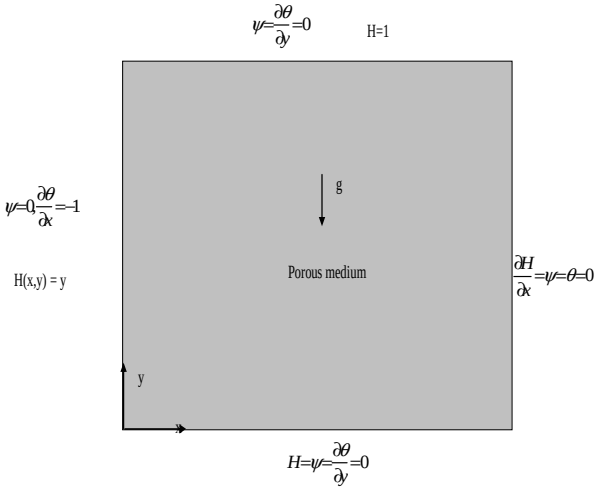

Fig. 1-b Dimensionless boundary conditions

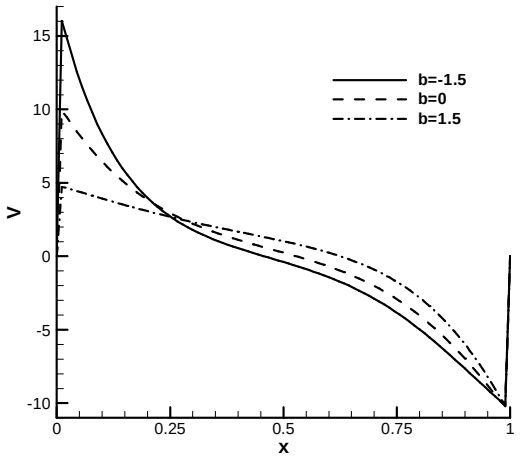

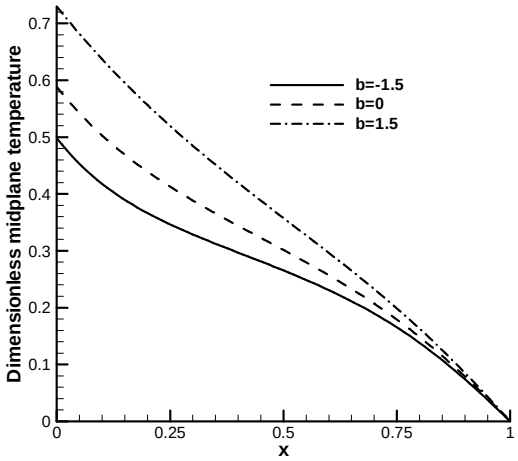

Fig 2 Horizontal mid-plane velocity (top) and temperature (bottom) for different values of b with Ra=50 and s=1000

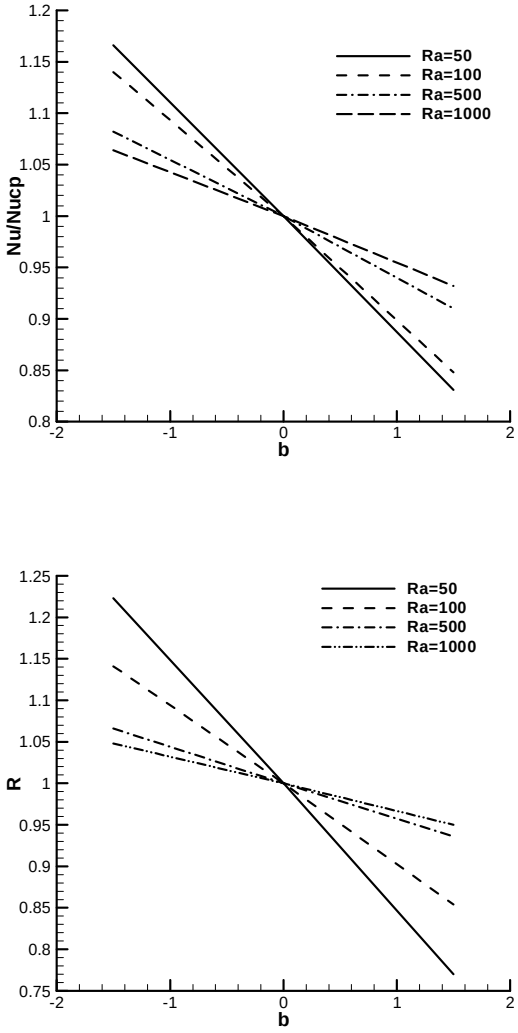

Fig 3 The variation of Nu/Nu_{cp} (top) and R (bottom) versus b with some values of Ra (s=100).

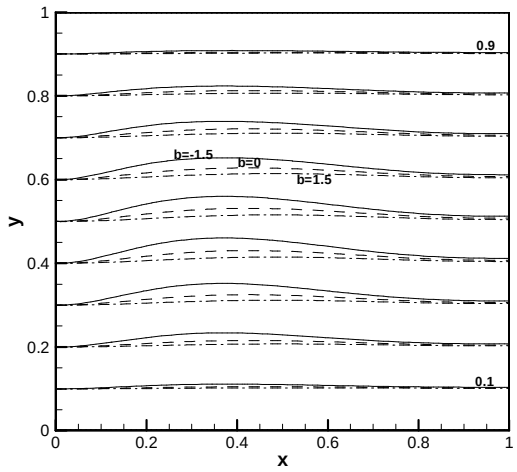

A

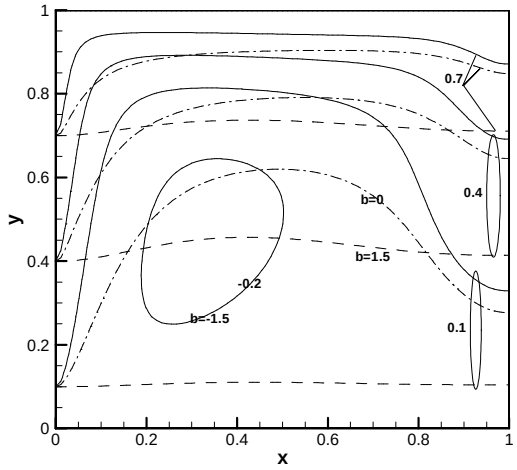

B

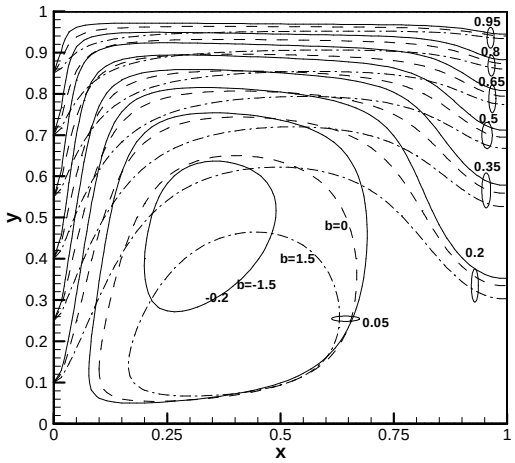

C

Fig 4 Heatlines for various b values with Ra=50 and A)s=1, B)s=100, and C) s=1000